



Contents lists available at ScienceDirect

Journal of Fluids and Structures

journal homepage: www.elsevier.com/locate/jfs

Suppression of the vortex-induced vibration of a circular cylinder surrounded by eight rotating wake-control cylinders

M. Silva-Ortega¹, G.R.S. Assi^{*,2}

Department of Naval Architecture & Ocean Engineering, EPUSP, University of São Paulo, São Paulo SP, Brazil

ARTICLE INFO

Article history:

Received 22 October 2016

Received in revised form 26 April 2017

Accepted 3 July 2017

Available online xxxx

Keywords:

Vortex-induced vibration

Suppression

Wake control

Drag reduction

ABSTRACT

The present work investigates the use of a polar array of 8 wake-control cylinders as a means of suppressing the vortex-induced vibration (VIV) of a larger circular cylinder. The diameter of the control cylinders and their rotation speed were the main parameters investigated. Experiments have been performed in water at Reynolds numbers between 5000 and 50,000. The rotating cylinders suppressed the peak amplitude of displacement by around 70% when compared to that of a bare cylinder. A similar response was obtained even if the rotation speed of the control cylinders was kept constant in relation to the flow speed. A specific configuration with 8 non-rotating control cylinders achieved an even better 99% suppression. As a consequence of reduced vibrations, the fluctuation of lift and mean drag were not as amplified due to VIV. The results pave the way for further studies concerning system optimization and support the development of efficient VIV suppressors and dynamic positioning systems for large floating offshore platforms and other applications.

© 2017 Elsevier Ltd. All rights reserved.

1. Introduction

Offshore platforms built to explore oil and gas in ultra-deep waters have become large floating units employed in almost all the processes of drilling, production and storage. Platforms of the mono-column and spar types present hulls in the form of a circular cylinder or other cylindrical shapes of bluff bodies, as reported by Gonçalves et al. (2010, 2011). Ocean currents past the hull will not only generate steady drag but also drive the platform into flow-induced motions that may affect the efficiency of the processes being carried out on the deck. Vibrations may also pose a threat to the structural integrity of the platform, of its mooring lines and riser pipes underwater (Sagrilo et al., 2009).

This type of flow-induced motion has its origin in the vortex-shedding mechanism of the flow past bluff bodies, which starts at the interaction of the separated shear layers in the near wake. Alternating vortices generate cyclic fluid loads (lift and drag) that feed back on the body. If the frequency of vortex shedding is approximate one of the natural frequencies of the elastic cylinder (f_0), the system will be excited into vortex-induced vibrations (VIV) for a wide range of flow speeds. Please refer to Bearman (1984) and Williamson and Govardhan (2004) for a detailed description of the phenomena involved.

Several strategies have been proposed to suppress VIV by disrupting the wake or avoiding the formation of vortices in the first place. Zdravkovich (1981) presented an introduction to some of those techniques, while Choi et al. (2008) reviewed different strategies to control the wake. With the advancement of control theory and its implementation, active strategies

* Corresponding author.

E-mail address: g.assi@usp.br (G.R.S. Assi).

¹ Now at the Dept. Naval Architecture, Universidad Veracruzana, Mexico.

² Currently a Visiting Associate in Aerospace at GALCIT, California Institute of Technology, USA.

to suppress VIV appeared with the promise of higher efficiency. From a phenomenological point of view, these techniques have to deal with very interesting (and complex) problems of unsteady hydrodynamics.

1.1. Flow control with interfering cylinders

It is known that the vortex-shedding mechanism of a circular cylinder can be controlled by the interference of small cylinders positioned around the circumference of the main body (Strykowski and Sreenivasan, 1990; Hwang and Choi, 2006). These wake-control cylinders interact with the boundary layer and the separated shear layers disrupting the formation of vortices that are convected downstream to form the wake. As a consequence, the cyclic hydrodynamic forces feeding back from the vortex-shedding mechanism are considerably reduced, if not completely suppressed. The mean drag acting on the body is also reduced if wake suppression is achieved.

Placing a smaller control cylinder upstream of the main cylinder is also a well-established strategy for drag reduction (Lee et al., 2004). But Strykowski and Sreenivasan (1990) have shown that if the small control cylinder is now placed within a defined region in the near wake, the formation of vortices could be effectively suppressed at a Reynolds number of $Re = 80$. Previous investigations positioning control cylinders in various arrangements around a bluff body have been performed through experiments and numerical simulations. Mittal (2001) performed numerical simulations of a static cylinder with two control cylinders positioned at $\pm 90^\circ$ in relation to the incoming flow. He found that vortex shedding was completely suppressed for a few arrangements at low Re .

Active open- and closed-loop control techniques have also received attention by the scientific community (Gad-El-Hak, 2000; Cattafesta and Sheplak, 2011; Schulmeister, 2012). Among them, the *moving surface boundary-layer control* (MSBC) method relies on the injection of momentum in the boundary layer by the rotation of small elements placed within or very near the boundary layer close to the separation points (Modi, 1997). Rotating elements are usually small circular cylinders placed inside or just above the wall. It is thought that the injection of momentum postpones the effects of the adverse pressure gradient, moving the separation points to a more advanced position. As a result, the wake becomes narrower and the recirculation region behind the body reduced. One of the most important control parameters directly associated with this technique is the ratio between the tangential velocity of the moving surface to the velocity of the free stream (U_c/U).

MSBC can be applied either as an active open- or closed-loop control strategy. Patnaik and Wei (2002) numerically simulated the flow around a D-section cylinder with MSBC at $Re = 200$ and 400 and verified a recirculation-free zone in the wake for $U_c/U = 1.25$. Muddada and Patnaik (2010) made further developments employing a cylinder fitted with two simple rotary type mechanical actuators located at 120° from the frontal stagnation point. The effectiveness of the MSBC in reducing drag was shown by all cases tested. Mittal and Raghuvanshi (2001) employed numerical simulations to observe that the control cylinders provided a local favorable pressure gradient in the wake region, thereby locally stabilizing the shear layers. Following that, Mittal (2001) applied the MSBC to control the flow around a circular cylinder in two-dimensional numerical simulations at $Re = 100$ and 10,000. At $Re = 100$ and $U_c/U = 5$, the flow achieved a steady state; at $Re = 10,000$ the wake did not reach a steady state, but it appeared highly organized and narrower when compared to the case without any control. The effect of the gap between the control cylinders and the wall of the main cylinder at $Re = 10,000$ was later investigated by Mittal (2003).

Korkischko and Meneghini (2012) performed an experiment employing MSBC with two wake-control cylinders as a means to suppress VIV of an isolated cylinder free to oscillate in the cross-flow direction ($Re \approx 7500$). They found that the two static control cylinders positioned at $\pm 90^\circ$ were not effective in suppressing VIV of the main body. However, when they applied enough rotation to the small cylinders, the wake was stabilized and VIV suppressed.

1.2. Objective

MSBC with more than two control cylinders has already been experimentally tested as a means to suppress vortex shedding of static cylinders as well as VIV of oscillating bodies (Silva-Ortega, 2015). Recently, Silva-Ortega et al. (2014b, a) have shown that a polar array of 2, 4 and 8 control cylinders equally spaced around a static body may create an effective device to suppress vortex shedding from a larger circular cylinder at $Re = 100$. Fundamental parameters (such as the number of control cylinders, their diameter and their distance from the main body) have been shown to play a significant role in the wake-control mechanism. Silva-Ortega (2015) also showed that the same arrays of control cylinders would impact the hydrodynamic loads acting on a static cylinder at $Re = 5000$ – $50,000$.

In a previous study, we have investigated the flow-induced vibration of a cylinder surrounded by a polar array of 2, 4 and 8 control cylinders that were not rotating (Silva-Ortega and Assi, 2017). That configuration was similar in nature to the axial-rods suppressors described by Zdravkovich (1981). It was found that, depending on the geometric configuration, the system could respond with a combination of VIV and galloping. In the present study, we will take the polar array with 8 control cylinders proposed by Silva-Ortega and Assi (2017) to control the wake of a static cylinder and employ it as a means of suppressing the VIV of a larger circular cylinder. This time, the 8 wake-control cylinders will be rotating (as in the MSBC technique) and the whole system will be free to respond to the flow excitation in the cross-flow direction. In this experiment, we expect to probe the parameter space regarding the dynamic response of the system to VIV.

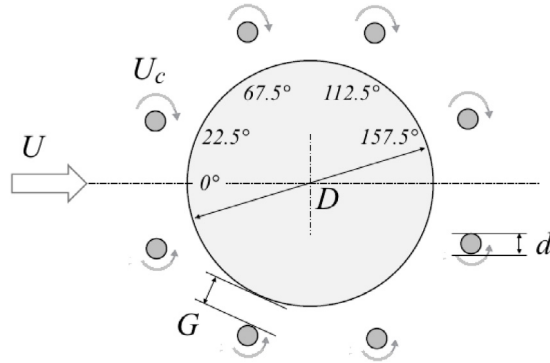


Fig. 1. Geometrical parameters for the main cylinder with eight control cylinders (figure not drawn to scale).

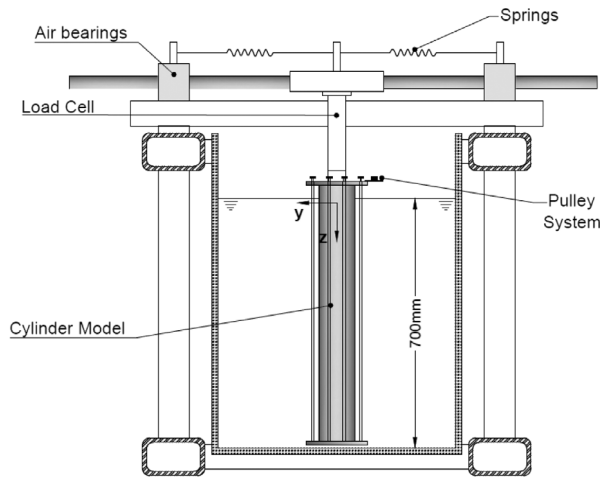


Fig. 2. Cross view of the experimental setup: elastic rig mounted on the test section.

2. Experimental setup

Experiments have been carried out in the Circulating Water Channel of NDF (Fluids and Dynamics Research Group) at the University of São Paulo, Brazil. The water channel has an open test section ($0.7 \text{ m} \times 0.9 \text{ m} \times 7.5 \text{ m}$) and good quality flow can be achieved up to 1 m/s with turbulence intensity of less than 3%.

A rigid section of a smooth circular cylinder was made of an acrylic tube of external diameter $D = 100 \text{ mm}$. Two sets of 8 control cylinders with diameter d were made of acrylic rods and supported by rings attached to the ends of the main cylinder. Their distribution about the main cylinder is presented in Fig. 1, in which the arrow indicates the direction of the incoming flow with velocity U . The axes of the control cylinders were parallel to the axis of the main cylinder, spanning the whole length of the model (immersed length of 700 mm). The diameter of the control cylinders was varied in two steps of $d/D = 0.06$ and 0.08 , while the gap measured between the wall of the control cylinders and the wall of the main cylinder was set to $G/D = 0.1$ in this study (based on the best results obtained by Silva-Ortega and Assi (2017)).

The top of the control cylinders was connected to a pulley system driven by an electric servo motor. All eight cylinders rotated at the same speed ratio U_c/U , where U_c is the tangential velocity on the wall of the control cylinders. As seen in Fig. 1, control cylinders at the top (starboard) rotated in the clockwise direction, while cylinders at the bottom (port) rotated in the opposite direction.

Models were mounted on a load cell attached to a sliding frame supported by air bearings, as shown in Fig. 2. A pair of coil springs provided the restoration force to the system, which was free to oscillate only in the cross-flow direction. An optical sensor measured the displacement (y) of the cylinder, providing that structural mass and damping were kept to a minimum. The product between the mass ratio (m^* , calculated as the ratio between the total oscillating mass and the mass of displaced water) and the damping ratio (ζ , measured as a percentage of the critical damping) was $m^*\zeta = 0.066$. The natural frequency of the system (f_0) as well as the damping ratio were determined during decay tests performed in air.

The only flow variable changed during the course of the experiments was the flow velocity, which altered the Reynolds number between 5000 and 50,000 ($Re = UD/\nu$, where ν is the kinematic viscosity of water) and the reduced velocity

Table 1
Parameters.

		1st series	2nd series	3rd series
Number of control cylinders	N	8		0, 8
Diameter of control cylinders	d/D		0.06, 0.08	
Gap between cylinders	G/D		0.1	
Rotation of control cylinders	U_c/U	1–10	0, 2, 2.5, 3	$U_c = 0.266$ m/s
Reynolds number	Re	10,500		5000–50,000
Reduced velocity	U_R	4.2		2–20
Mass ratio	m^*		1.09	
Damping ratio	ζ		0.61%	

$U_R = U/(Df_0)$ in the range of 2 to 20. A summary of all the parameters investigated in the experiments is presented in Table 1. The dynamic responses to VIV are analyzed across the U_R range by comparing the normalized amplitude of displacement (\hat{y}/D , where \hat{y} is the RMS of y times $\sqrt{2}$), the dominant frequency of oscillation normalized by the natural frequency (f/f_0), the mean drag coefficient (\bar{C}_D) and the RMS of the lift coefficient (\hat{C}_L). In addition, preliminary tests have been performed with a bare cylinder (without control cylinders) to serve as reference for comparison.

2.1. Method

As reported by Silva-Ortega and Assi (2017), we have started this VIV research project testing 27 different cases varying the parameters N , d/D and G/D for a cylinder surrounded by non-rotating control cylinders. Each case was run for a whole range of reduced velocities, resulting in a series of VIV response curves. Now, in order to investigate the effect of the rotating cylinders one needs to add the new parameter U_c/U . If U_c/U were to be varied in ten steps, say between 1 and 10, one would end up with another 270 cases to test over the same reduced velocity range.

To avoid an exhaustive investigation of the parametric space, our current work took the most effective case for VIV suppression with non-rotating control cylinders found by Silva-Ortega and Assi (2017) to investigate its behavior for rotating control cylinders. The chosen configuration had $N = 8$ control cylinders, $d/D = 0.08$ (with one extra variation) and $G/D = 0.1$. The present investigation was divided into three series of experiments concerning the most significant parameters expected to govern the phenomenon:

1st series: We chose configurations with $d/D = 0.06$ and 0.08 to investigate the dependency of the peak response at the VIV resonance to the rotation speed of the control cylinders. U_c/U was varied in smaller intervals to probe which rotation speed would produce the most suppression at $U_R = 4.2$.

2nd series: We took the best case for peak suppression found in the first series and varied the whole range of U_R keeping U_c/U constant. Since U was increased to change U_R , the actual rotation of the control cylinders (U_c) was also increased in order to keep U_c/U constant.

3rd series: We set out to investigate the effectiveness of VIV suppression if the actual rotation speed U_c was kept constant for the whole range of U_R , thus altering the ratio U_c/U for each step of U . For that matter, the value of U_c that produced the best peak suppression in the first series was employed.

3. Results and discussion

The parametric variation for each series of experiments is also presented in Table 1. We shall now turn to their results.

3.1. 1st series: peak amplitude at $U_R = 4.2$

In addition to the case with $d/D = 0.08$, one extra variation was tested with a smaller diameter of $d/D = 0.06$ (both cases kept a radial separation of $G/D = 0.1$). Numerical simulations of the flow performed by Silva-Ortega et al. (2014a) have shown that a rotation speed of $U_c/U = 3$ was enough to control vortex shedding of a static cylinders for low Re . Based on that, we varied U_c/U in small intervals from 1 to 9. The reduced velocity was kept constant at $U_R = 4.2$ (equivalent to $Re = 10,500$), which corresponded to the point of maximum amplitude for the bare cylinder at the VIV resonance (to be discussed later).

Fig. 3 presents the peak amplitude of response versus U_c/U for both cases with $d/D = 0.08$ and 0.06 . The lowest value of $[\hat{y}/D]_{\text{peak}} \approx 0.2$ was found at $U_c/U = 2.5$ for both cases. For lower and higher rotation speeds the peak response was considerably increased. Consequently, $U_c/U = 2.5$ and its neighboring values of $U_c/U = 2$ and 3 were chosen as the reference values to proceed to the second series of experiments.

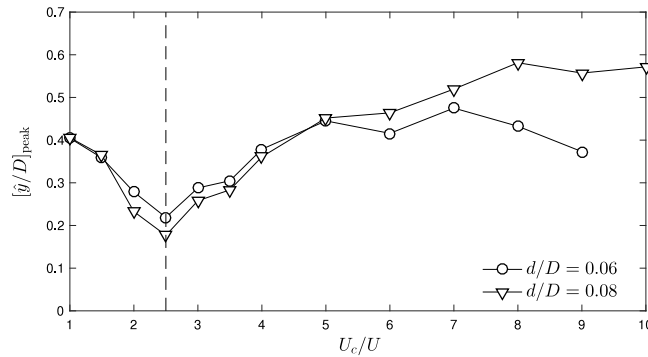


Fig. 3. Peak amplitude of response varying U_c/U at $U_R = 4.2$ and $Re = 10,500$.

3.2. 2nd series: VIV response for $U_c/U = 2, 2.5$ and 3

A preliminary experiment with a bare cylinder (without surrounding control cylinders) has been performed to validate the setup and generate the reference data for comparison. Fig. 4 shows the reference case obtained for reduced velocities up to 20. The results of VIV amplitude of displacement, frequency of oscillation, mean drag coefficient and fluctuating lift coefficient obtained for the bare cylinder are in good agreement with other experimental results collected by Williamson and Govardhan (2004), Norberg (2003) and Assi et al. (2013), who also employed the same apparatus. The reference results for a cylinder with 8 non-rotating control cylinders ($U_c/U = 0$) have been extracted from Silva-Ortega and Assi (2017).

Fig. 4 shows the amplitude of displacement (\hat{y}/D), frequency of oscillation (f/f_0), mean drag coefficient (\bar{C}_D) and RMS of lift coefficient (\hat{C}_L) for the case with $d/D = 0.08$ with varying U_c/U versus reduced velocity. The response curve for the bare cylinder is in clear contrast with the curves of the rotating cylinders (Fig. 4(a)). In general, all rotation speeds managed to reduce the amplitude of VIV in the initial, upper and lower branches (as defined by Williamson and Govardhan (2004)). At $U_R = 4.2$, the peak responses match those presented in Fig. 3. (Please note that the data points do not cover the whole range of U_R up to 20. Since the actual rotation speed (U_c) of the control cylinders was increasing with U_R , the motor reached its maximum rotation speed limiting the experiment to $U_R \approx 12$.)

The case with $U_c/U = 2.5$ presented the lowest response for the widest range of U_R , but the other two neighboring cases also showed similar responses. The striking result, however, came out when the responses were compared with that for 8 non-rotating cylinders: A cylinder surrounded by 8 non-rotating cylinders ($U_c/U = 0$) appeared to offer considerably better suppression than the cases with rotating cylinders. For the whole range of U_R , the case with non-rotating cylinders rarely passed $\hat{y}/D = 0.1$, while the rotating cylinders reached $\hat{y}/D \approx 0.25$ during the synchronization range. The non-rotating wake-control cylinders appear to be more efficient in suppressing VIV, at least for this set of parameters.

The frequency of response presented in Fig. 4(b) clearly shows that the bare cylinder and the cylinder with rotating cylinders all follow the expected behavior for VIV. The data points representing the dominant f/f_0 follow closely the $St = 0.2$ line (the inclined line representing the typical Strouhal number for a circular cylinder). The dominant frequency for $U_c/U = 0$, on the other hand, shows that the system only oscillated at very low frequencies, associated with slow drifts at small displacements.

As a consequence of the VIV suppression, \bar{C}_D presented in Fig. 4(c) shows considerably low values for the case with $U_c/U = 0$. When the control cylinders are rotating, mean drag is increased above the value found for the bare cylinder, considerably higher than the mean drag for the case with non-rotating cylinders. Fig. 4(d) also reveals that the rotating cylinders generate more lift driving the excitation, when compared with the results for the non-rotating cylinders.

The same experiment was repeated for smaller control cylinders with $d/D = 0.06$, as seen in Fig. 5. Again, the cases with rotating cylinders showed a considerable reduction of response when compared with that of the bare cylinder. Maximum response for the case with $U_c/U = 2.5$ reached $\hat{y}/D \approx 0.25$ during the synchronization range. The frequency response, as well as the curves of \bar{C}_D and \hat{C}_L , show a similar behavior.

The unexpected response now appeared for the case with non-rotating control cylinders. Instead of suppressing VIV for the whole range of U_R , the case with slightly smaller control cylinders ($d/D = 0.06$) presented a peak response of $\hat{y}/D \approx 0.5$ at the resonance. This is worse than the displacement measured for the cases with rotating cylinders. In fact, it appears that the VIV mechanism could not be suppressed as before, but only restricted to a shorter range of U_R . Fig. 5(b) shows a dominant frequency signature over the Strouhal line, indicating that the fundamental mechanisms are not different from VIV. In spite of reducing the peak amplitude of vibration, the rotating cylinders still presented \bar{C}_D higher than that of non-rotating cylinders for the whole U_R range; for most of the time it was also higher than that of a bare cylinder.

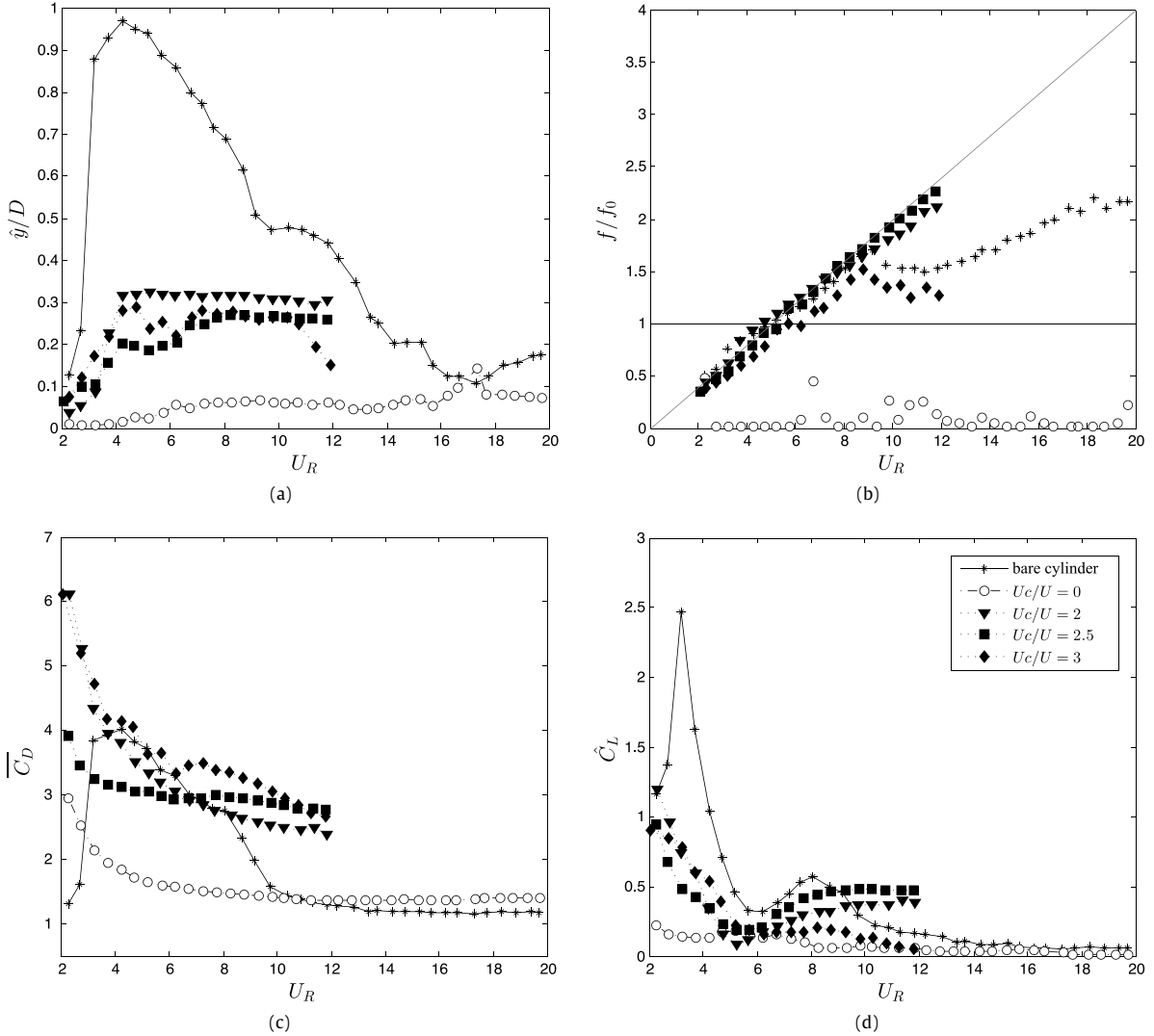


Fig. 4. VIV response for 8 control cylinders with $d/D = 0.08$ at $U_c/U = 0, 2, 2.5$ and 3 : (a) Amplitude of displacement, (b) frequency of oscillation, (c) mean drag and (d) RMS of lift coefficients.

3.3. 3rd series: VIV response for $U_c = 0.266$ m/s

In the third series, the actual rotation of the control cylinders (U_c) was kept constant independently of the flow speed (U), thus altering the ratio U_c/U as U_R was increased. The value of $U_c = 0.266$ m/s was chosen because it was the actual rotation speed at the peak-amplitude during the first series of experiments; i.e. $U_c = 0.266$ m/s resulted in $U_c/U = 2.5$ for $U_R = 4.2$. Keeping U_c constant resulted in a variation of $U_c/U = 5.25$ – 0.52 for the range of $U_R = 2$ – 20 , since both parameters vary inversely to each other, but linearly with flow speed.

At a constant U_c , the reduced velocity range could now be extended up to $U_R = 20$. Results for both cases with $d/D = 0.08$ and 0.06 are compared with those of the bare cylinder, the non-rotating control cylinders ($U_c/U = 0$) and the rotating cylinders with $U_c/U = 2.5$ discussed in the second series.

The amplitude of displacement presented in Fig. 6(a) reveals that both cases with rotating control cylinders managed to reduce the VIV response in the synchronization range. But the residual vibration of $\hat{y}/D > 0.2$ is still worse than the suppression achieved by the non-rotating cylinders ($U_c/U = 0$). (Please note that both curves match at $U_R = 4.2$ in all plots of Fig. 6, as expected.)

With $U_c = 0.266$ m/s, U_R was extended to 20, revealing a drop in the \hat{y}/D curve at $U_R \approx 12$, marking the end of the synchronization range (also noticeable in the frequency signature of Fig. 6(b)). It is important to note that the system was not induced into other types of vibration for higher flow speeds, such as galloping or turbulence buffeting.

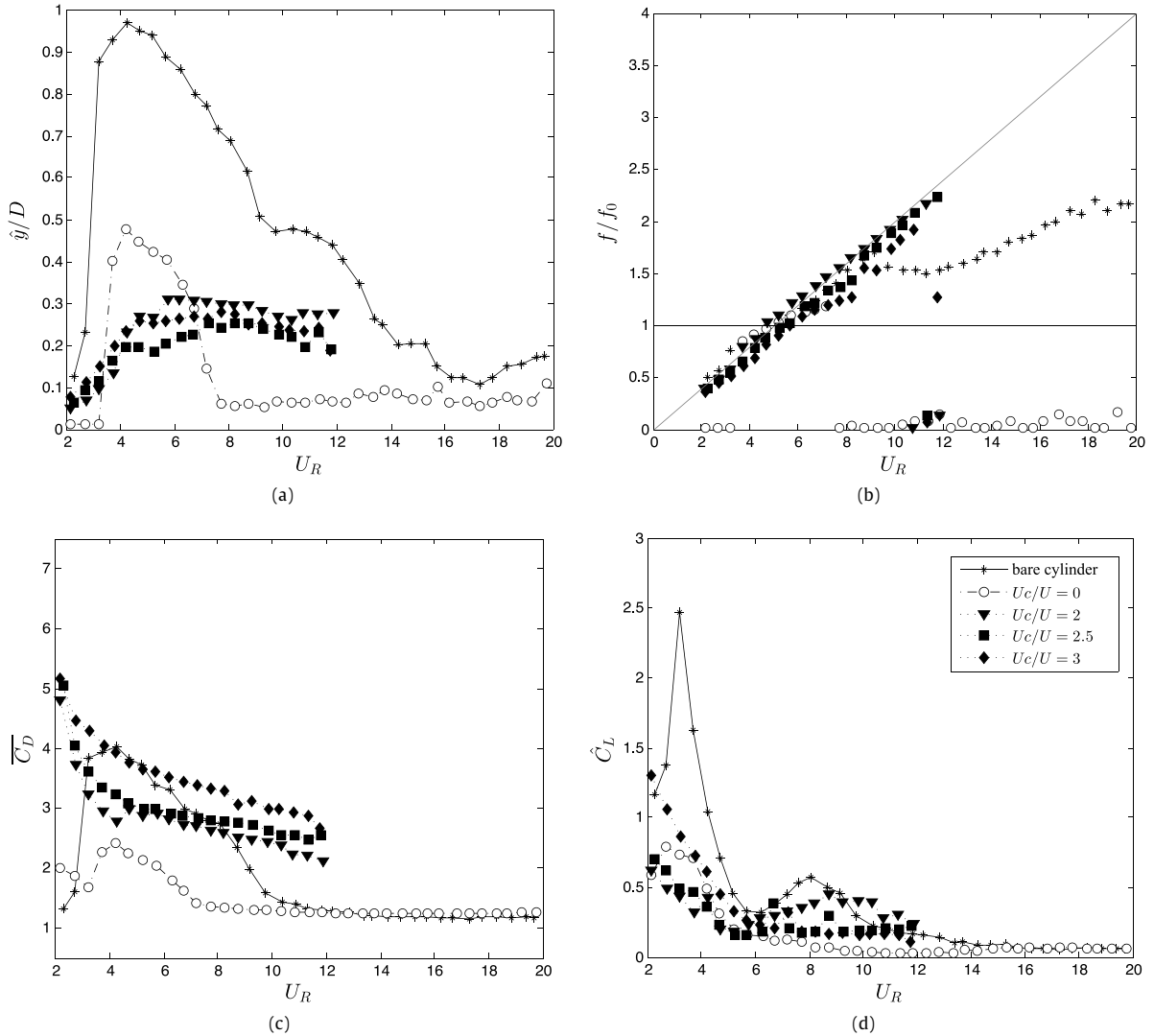


Fig. 5. VIV response for 8 control cylinders with $d/D = 0.06$ at $U_c/U = 0, 2, 2.5$ and 3 : (a) Amplitude of displacement, (b) frequency of oscillation, (c) mean drag and (d) RMS of lift coefficients.

Mean drag and RMS of lift show the similar pattern seen before. Although the case with $U_c = 0.266$ m/s presented a decrease in \bar{C}_D for higher reduced velocities (Fig. 6(c)), it did not reduce drag below the value measured for non-rotating control cylinders. As expected, \bar{C}_D was below that of a bare cylinder during synchronization, but larger thereafter.

Fig. 7 shows a slight improvement in the response if the control cylinders with $d/D = 0.06$ are rotated at $U_c = 0.266$ m/s, when compared with the previous case with $d/D = 0.08$: the synchronization range is shortened, but the maximum displacement is kept at the same level of $\hat{y}/D \approx 0.35$ (Fig. 7(a)).

As happened before, the rotating control cylinders produced better suppression than the non-rotating cylinders ($U_c/U = 0$), but with the cost of increasing drag for a wider range of reduced velocities (Fig. 7(c)). For $U_R > 10$, the cases with $U_c/U = 0$ and $U_c = 0.266$ m/s were able to reach the lowest values of mean drag recorded for the bare cylinder beyond the synchronization range ($\bar{C}_D \approx 1.4$).

3.4. Discussion of all three series

As a first general comment, it is important to highlight that the VIV suppression achieved by an array of 8 non-rotating control cylinders ($U_c/U = 0$) with $d/D = 0.08$ was higher than any other case investigated in the present work. Consequently, mean drag was also reduced to the minimum observed value. Indeed, only by positioning the non-rotating control cylinders around the main cylinder was enough to achieve an almost 99% suppression of the peak amplitude of

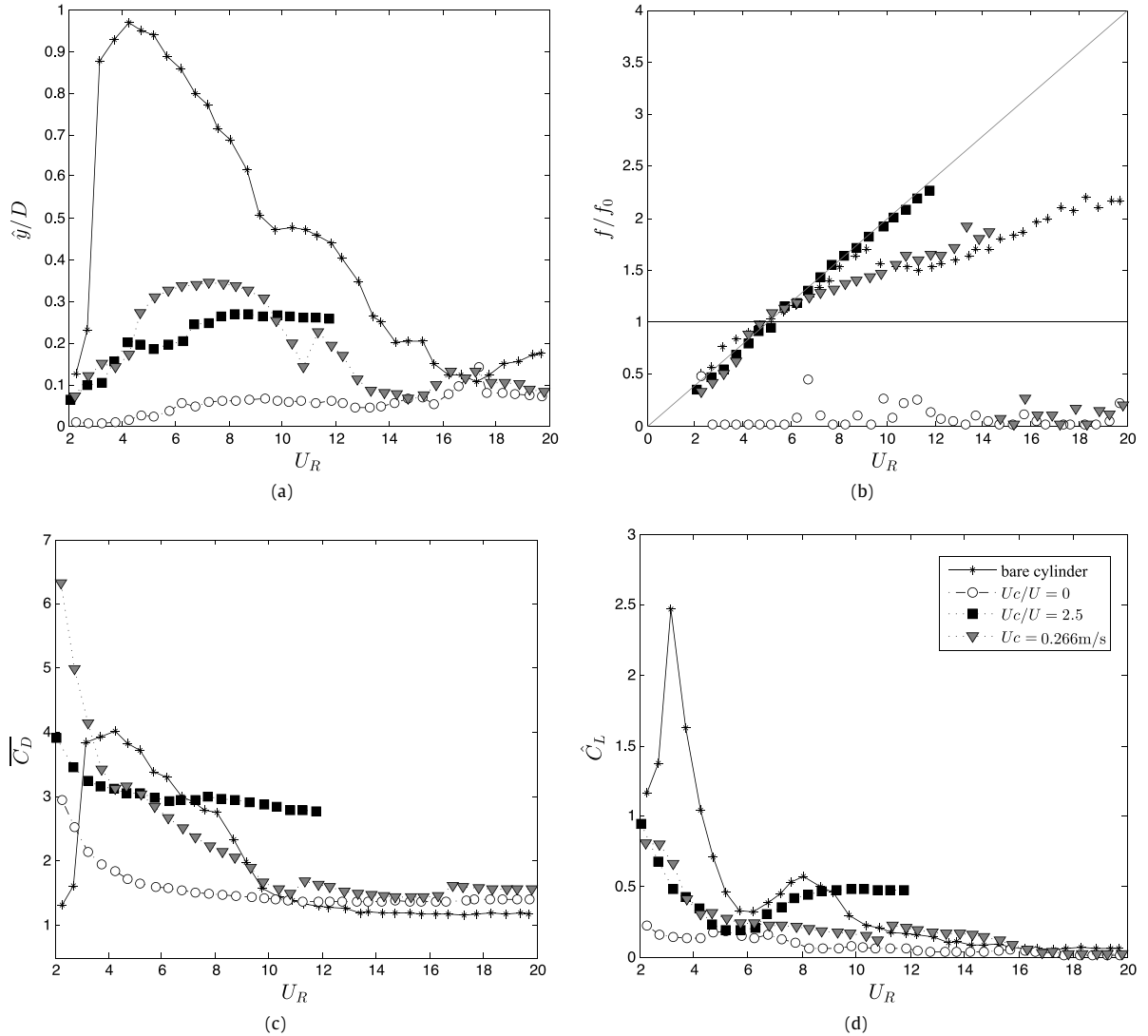


Fig. 6. VIV response for 8 control cylinders with $d/D = 0.08$ at $U_c = 0.266$ m/s: (a) Amplitude of displacement, (b) frequency of oscillation, (c) mean drag and (d) RMS of lift coefficients.

displacement at resonance (Fig. 4). This arrangement, however, proved to be very sensitive to the position and the diameter of the control cylinders. A small reduction to $d/D = 0.06$ would make the non-rotating cylinders suppress only roughly 50% of the peak amplitude of displacement (Fig. 5). This result invites further investigation of the hydrodynamic mechanisms between the control cylinders and the boundary layer.

Now, when the cylinders (with either $d/D = 0.08$ or 0.06) were allowed to rotate, the system consistently reached approximately 70%–75% of VIV suppression at resonance, also becoming less susceptible to small variations in the d/D parameter. In brief, the rotating cylinders may not provide the very best performance, but certainly a more predictable suppression.

Differently from the results reported by Korkischko and Meneghini (2012), who employed two rotating control cylinders at $\pm 90^\circ$ ($d/D = 0.06$, $G/D = 0.07$ and $U_c/U = 5$ – 25), our cases with 8 rotating cylinders did not achieve the same level of VIV suppression and drag reduction. Although Korkischko and Meneghini (2012) applied much higher rotation speeds to their cylinders, we do not believe that the total rotation (or sum of angular momentum transferred to the flow) is the only parameter to govern the suppression. The position and size of the control cylinders indeed play a significant role, as supported by previous studies on the sensibility of wakes (Strykowski and Sreenivasan, 1990; Patino et al., 2015, 2017) together with our results for $U_c/U = 0$ (that managed to stabilize the wake with no rotation).

In general, the behavior of the response found when the 8 control cylinders were rotating was qualitatively the same for all configurations. Since the second series was based on the best results of the first series ($U_c/U = 2.5$) – for higher and

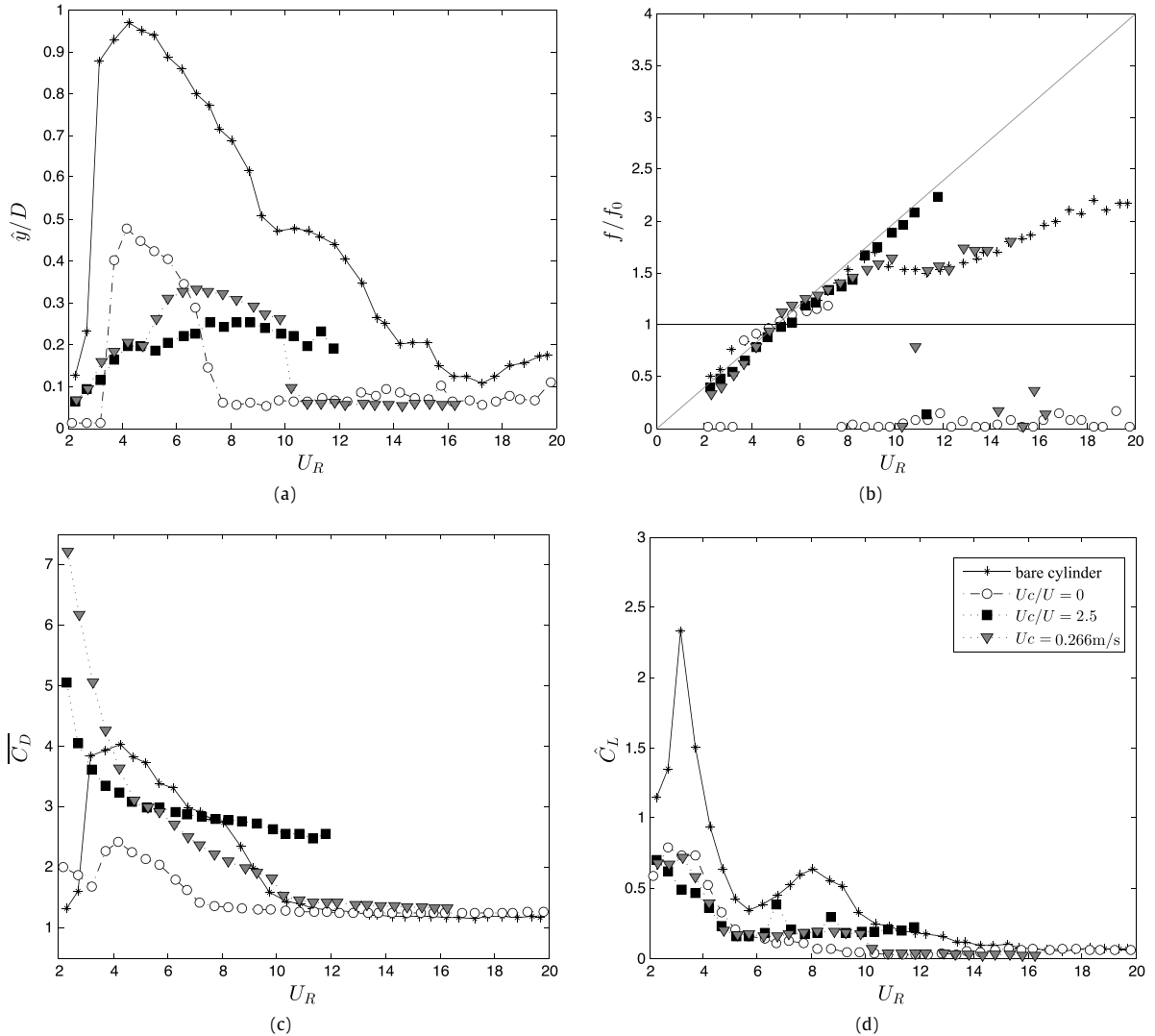


Fig. 7. VIV response for 8 control cylinders with $d/D = 0.06$ at $U_c = 0.266$ m/s: (a) Amplitude of displacement, (b) frequency of oscillation, (c) mean drag and (d) RMS of lift coefficients.

lower rotation speeds ($U_c/U = 2$ and 3) the peak amplitude was found to be higher —, we believe that the response curves for rotating cylinders with $U_c/U \neq 2.5$ should not produce better results, at least not for this range of Re .

If rotation is to be applied, the question would turn to the optimum rotation speed. The optimum U_c is most certainly a function of U , since the vortex shedding mechanism by which the cylinders are actuating depends on Reynolds number. But if it were not necessary to correct U_c for each flow speed, the control strategy for this kind of suppression device would be significantly simplified. Since this study is not concerned with optimization, we have limited the investigation to keeping a constant U_c .

As seen in Figs. 6 and 7, keeping a constant actual rotation of $U_c = 0.266$ m/s (which corresponded to $U_c/U = 2.5$ at $U_R = 4.2$) did not change the response significantly. It is possible that an optimized rotation speed would produce better suppression at the new peak of response (around $U_R = 7$ in Figs. 6(a) and 7(a)), but one is left to wonder if it would be worth implementing this kind of closed-loop control in a practical application. This is an interesting topic for further investigations.

4. Further discussion and future work

The present investigation showed that the classical axial rods are not a bad suppressor after all, given that their geometry (density, distribution, etc.) is correct. For certain conditions, a simple array of non-rotating control cylinders in the form of axial rods might achieve satisfactory suppression. If the operator can live with the difference in peak amplitude between

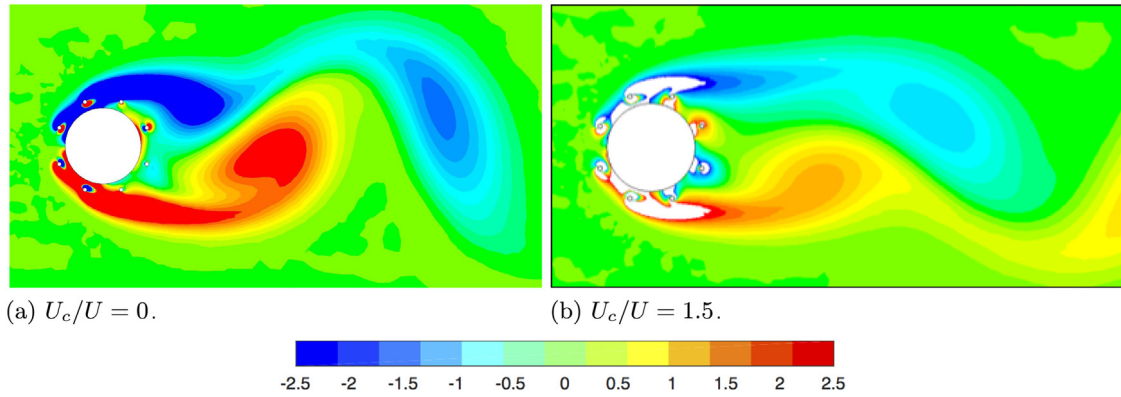


Fig. 8. Instantaneous vorticity contours (s^{-1}); $d/D = 0.05$, $G/D = 0.1$ and $Re = 100$.
Source: Reproduced from Silva-Ortega et al. (2014a).

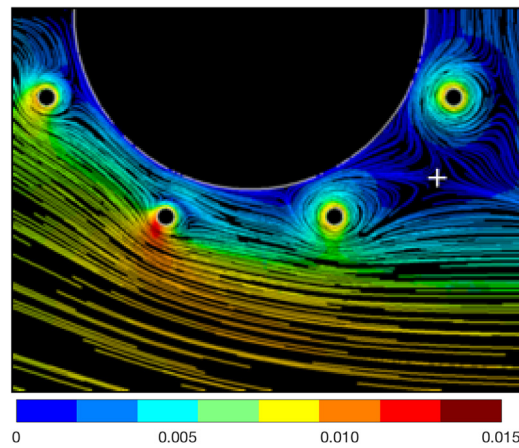


Fig. 9. Detail of the streamlines around the rotating control cylinders of Fig. 8(b). Flow is from left to right; colored by velocity magnitude (m/s). (For interpretation of the references to color in this figure legend, the reader is referred to the web version of this article.)
Source: Reproduced from Silva-Ortega et al. (2014a).

0.25 and 0.5, it might be better to stick to the non-rotating cylinders as far as drag is concerned. Now if vibration is to be reduced at any drag cost, say to avoid fatigue damage or dynamic loads, then the rotating cylinders could be considered as an option. In a floating offshore platform with a bluff-body hull (a mono-column or a spar platform, for example), it might be desirable to mitigate vibration and the dynamic loads associated with it even if the mooring lines are to be loaded with extra drag.

If the main cylinder were a static body, the rotation of the control cylinders could help to suppress the wake and reduce loads due to vortex shedding, as shown by Silva-Ortega (2015). But rotating cylinders may not produce the expected result of VIV suppression with drag reduction if the cylinder is free to respond to the flow (this is true for this range of Re). Again, this is proof that if a device appears to reduce hydrodynamic loads on a static body it does not necessary mean that it will make a good VIV suppressor, especially if the system presents low mass and damping. It might be the case that for a system with higher $m^*\zeta$, a suppressor with 8 rotating cylinders could present a qualitatively different response.

Of course there are infinite possibilities to arrange and drive the rotating control cylinders around the main cylinder. The present work was never intended to find an optimal solution to the problem, but simply to probe a finite parametric space. For a serious optimization study this space is so vast that a robust optimization method must be considered to tackle the problem, especially if each of the control cylinders had an independent U_c . So many possibilities make it a very exciting, non-linear optimization problem for future investigations.

The most interesting question about the hydrodynamic mechanisms caused by the 8 control cylinders remains unanswered. Some light has been shed from numerical simulations of the flow performed by Silva-Ortega et al. (2014a). Fig. 8 compares the results of two-dimensional numerical simulations of the flow around static cylinders with 8 rotating control cylinders with $U_c/U = 0$ and 1.5 at $Re = 100$. Even though Re was significantly lower, it was possible to notice that the rotating control cylinders not only produced weaker vortices, but a narrower wake with an almost doubled vortex-formation

length. A closer look at the streamlines around the control cylinders on one of the sides (presented in Fig. 9) reveals the existence of reversed flow near the wall of the main cylinder. This might be causing the global separation point (marked by a cross on a saddle region of the streamlines) to offset from the wall of the main cylinder in between the third and the fourth control cylinders. The momentum transferred from the control cylinders might help the flow to better withstand the adverse pressure gradient, delaying separation.

The interaction between the control cylinders and the boundary layer must be strongly depend on Re , especially for Re approaching the transition from a laminar to a turbulent regime of the boundary layer. In the present experiments, for example, we were not able to evaluate if the control cylinders were immersed or outside of the boundary layer, as suggested by Silva-Ortega et al. (2014a) for $Re = 100$. In order to better evaluate the governing hydrodynamic mechanisms at higher Re , further investigations employing flow visualization and detailed PIV of the near wake and around the control cylinders are planned in the near future.

Finally, the behavior of the wake for oscillating cylinders under VIV is of particular interest, since the angle of attack of the incoming flow relative to the control cylinders will vary through the cycle of vibration. It is possible that the relative angle of attack due to the body's cross-flow velocity causes the frontal stagnation point to approach one of the control cylinders. If that occurs, say at an instant of the oscillation cycle, the wake could present unsteady variations in its dynamics. We believe that an arrangement that produces a control cylinder at the stagnation point would break the symmetry of the flow, resulting in a non-symmetric wake that could result in a steady lift force to one of the sides. This topic should be pursued in future experiments.

5. Conclusion

Amplitude of response, frequency of oscillations, mean drag and fluctuating lift coefficients were measured for two configurations of a device made with 8 rotating control cylinders employed to suppress the VIV of a main circular cylinder. Results were obtained for three different values of the rotation parameter (U_c/U) and, finally, with a constant tangential velocity (U_c) between $Re = 5000$ and $50,000$.

Both configurations (with $d/D = 0.08$ and 0.06) reduced the peak amplitude of response in about 70% when compared with that of a bare cylinder for a rotation speed of $U_c/U = 2.5$. A similar reduction was found when the tangential velocity remained constant at $U_c = 0.266$ m/s across the range of reduced velocities. Nevertheless, as far as VIV suppression and drag reduction were concerned, the best case overall was found for the configuration with 8 non-rotating control cylinders, ($d/D = 0.08$ with $G/D = 0.10$ and $U_c/U = 0$), achieving approximately a 99% suppression of the peak displacement at the VIV resonance.

In general, the RMS of lift was also minimized by all configurations. Measurements have shown that these configurations with 8 control cylinders do not reduce the mean drag coefficient as much as the case with 2 rotating control cylinders reported in the experimental investigation of VIV by Korkischko and Meneghini (2012) and in the numerical simulations of a static cylinder performed by Mittal (2001). In terms of efficiency, the case with a constant tangential velocity (U_c) performed better than with a constant rotation ratio (U_c/U) along the reduced velocity range. The peak amplitude of displacement was not very different between the two cases, but the constant U_c would require less energy to drive the 8 control cylinders as flow speed was increased.

An explanation for the hydrodynamic mechanisms around the control cylinders and in the near wake is still required.

Acknowledgments

MSO is grateful to CAPES Brazilian Ministry of Education. GRSA acknowledges the support of FAPESP (2011/00205-6, 2014/50279-4), CNPq (306917/2015-7) and the Brazilian Navy.

References

- Assi, G.R.S., Bearman, P.W., Carmo, B.S., Meneghini, J.R., Sherwin, S.J., Willden, R.H.J., 2013. The role of wake stiffness on the wake-induced vibration of the downstream cylinder of a tandem pair. *J. Fluid Mech.* 718, 210–245.
- Bearman, P.W., 1984. Vortex shedding from oscillating bluff bodies. *Ann. Rev. Fluid Mech.* 16, 195–222.
- Cattafesta, L.N., Sheplak, M., 2011. Actuators for active flow control. *Annu. Rev. Fluid Mech.* 43, 247–272.
- Choi, H., Jeon, W.-P., Kim, J., 2008. Control of flow over a bluff body. *Annu. Rev. Fluid Mech.* 40, 113–139.
- Gad-El-Hak, M., 2000. *Flow Control: Passive, Active, and Reactive Flow Management*. Cambridge University Press.
- Gonçalves, R.T., Fajarra, A.L.C., Rosetti, G.F., Nishimoto, K., 2010. Mitigation of vortex-induced motion (VIM) on a monocolumn platform: forces and movements. *J. Offshore Mech. Arctic Eng.* 132 (4), 041102.
- Gonçalves, R.T., Rosetti, G.F., Fajarra, A.C., Nishimoto, K., 2011. An overview of relevant aspects on VIM of spar and monocolumn platforms. *J. Offshore Mech. Arctic Eng.* 134 (1), 014501.
- Hwang, Y., Choi, H., 2006. Control of absolute instability by basic-flow modification in a parallel wake at low Reynolds number. *J. Fluid Mech.* 560, 465–475.
- Korkischko, I., Meneghini, J.R., 2012. Suppression of vortex-induced vibration using moving surface boundary-layer control. *J. Fluids Struct.* 34, 259–270.
- Lee, S.-J., Lee, S.-I., Park, C.-W., 2004. Reducing the drag on a circular cylinder by upstream installation of a small control rod. *Fluid Dyn. Res.* 34 (4), 233–250.
- Mittal, S., 2001. Control of flow past bluff bodies using rotating control cylinders. *J. Fluids Struct.* 15 (2), 291–326.
- Mittal, S., 2003. Flow control using rotating cylinders: effect of gap. *J. Appl. Mech.* 70 (5), 762–770.
- Mittal, S., Raghuvanshi, A., 2001. Control of vortex shedding behind circular cylinder for flows at low Reynolds numbers. *Internat. J. Numer. Methods Fluids* 35 (4), 421–447.

- Modi, V.J., 1997. Moving surface boundary-layer control: A review. *J. Fluids Struct.* 11 (6), 627–663.
- Muddada, S., Patnaik, B.S.V., 2010. An active flow control strategy for the suppression of vortex structures behind a circular cylinder. *Eur. J. Mech. B Fluids* 29 (2), 93–104.
- Norberg, C., 2003. Fluctuating lift on a circular cylinders: Review and new measurements. *J. Fluids Struct.* 17, 57–96.
- Patino, G., Silva-Ortega, M., Gioria, R.S., Assi, G.R.S., Meneghini, J.R., 2015. Investigation of circular-cylinder VIV passive-control device using flow sensitivity analysis. In: *Bifurcations and Instabilities in Fluid Dynamics, BIFD2015*, France.
- Patino, G.A., Gioria, R.S., Meneghini, J.R., 2017. Evaluating the control of a cylinder wake by the method of sensitivity analysis. *Phys. Fluids* 29 (4), 044103.
- Patnaik, B.S.V., Wei, G.W., 2002. Controlling wake turbulence. *Phys. Rev. Lett.* 88, 1–4.
- Sagrilo, L.V.S., Siqueira, M.Q., Lacerda, T.A.G., Ellwanger, G.B., Lima, E.C.P., Siqueira, E.F.N., 2009. VIM and wave-frequency fatigue damage analysis for SCRs connected to monocolumn platforms. In: *ASME 2009 28th International Conference on Ocean, Offshore and Arctic Engineering, OMAE2009-79807*, pp. 723–729.
- Schulmeister, J.C., 2012. *Flow Separation Control with Rotating Cylinders* (Master's thesis), Massachusetts Institute of Technology.
- Silva-Ortega, M., 2015. *Suppression of Vortex-Induced Vibration of a Circular Cylinder with Fixed and Rotating Control Cylinders* (Master's thesis), University of São Paulo, Available at www.teses.usp.br.
- Silva-Ortega, M., Assi, G.R.S., 2017. Flow-induced vibration of a circular cylinder surrounded by two, four and eight wake-control cylinders. *Exp. Therm. Fluid Sci.* 85, 354–362.
- Silva-Ortega, M., Orselli, R.M., Assi, G.R.S., 2014a. Control of rotating cylinders as suppressors of vortex-induced vibration of a bluff body. In: *Proceedings of SOBENA2014 the 25th Congress of the Brazilian Society of Naval Architects, SOBENA*.
- Silva-Ortega, M., Orselli, R.M., Assi, G.R.S., 2014b. Control of vortex shedding of a circular cylinder with two and four small rotating cylinders. In: *Proceedings of EPTT2014 the XI Spring School of Turbulence and Transition. ABCM*.
- Strykowski, P.J., Sreenivasan, K.R., 1990. On the formation and suppression of vortex shedding at low Reynolds numbers. *J. Fluid Mech.* 218, 71–107.
- Williamson, C.H.K., Govardhan, R., 2004. Vortex-induced vibrations. *Ann. Rev. Fluid Mech.* 36, 413–455.
- Zdravkovich, M.M., 1981. Review and classification of various aerodynamic and hydrodynamic means for suppressing vortex shedding. *J. Wind Eng. Ind. Aerodyn.* 7, 145–189.